Melittin promotes the proliferation of Schwann cells in hyperglycemic environment by up-regulating the Crabp2/Wnt/β-catenin signaling pathway

QIUYI ZHANG[1*], YUXIA CHEN[1*], WEI HUANG[1], JIAQIAN ZHOU[1] and DAWEI YANG[2]

[1]National Immunological Laboratory of Traditional Chinese Medicine Affiliated to Youjiang Medical College for Nationalities, Baise, Guangxi Zhuang Autonomous Region 533000, P.R. China; [2]Department of Gerontology, Affiliated Hospital of Youjiang Medical University for Nationalities, Baise, Guangxi Zhuang Autonomous Region 533099, P.R. China

Received July 3, 2024; Accepted August 29, 2024

DOI: 10.3892/mmr.2024.13371

Abstract. The present study aimed to explore the effect of melittin (MLT) on the growth of Schwann cells (SCs) in high glucose conditions and to understand the mechanisms involved. The goal was to provide a theoretical basis for using MLT in the treatment of diabetic peripheral neuropathy (DPN). The CCK-8 assay was used to measure cell activity at different concentrations of glucose and MLT. Flow cytometry was employed to analyze the effect of MLT on cell cycle phases and apoptosis in SCs under high glucose conditions. To identify differentially expressed proteins, 4D label-free quantitative proteomics with liquid chromatography-mass spectrometry was used, followed by biological analysis to explore potential mechanisms. PCR, western blotting and immunofluorescence were conducted to confirm these mechanisms. Melittin (0.2 μg/ml) increased the proliferation of SCs in a high glucose environment. Flow cytometry showed that after MLT treatment, the proportion of cells in the G_2/M+S phase increased and the combined ratio of early and late apoptosis decreased under high glucose conditions. Proteomics identified 1,784 proteins with significant changes in expression; 725 were upregulated, and 1,059 were downregulated. Kyoto Encyclopedia of Genes and Genomes analysis indicated that the differentially expressed proteins were mainly involved in metabolic pathways and neurodegenerative disease pathways. PCR, western blotting and immunofluorescence confirmed the increase in Crabp2, Wnt3a, C-Jun, CDK4, CyclinD1 and proliferating cell nuclear antigen. In high glucose conditions, MLT protects SCs from glucose toxicity by upregulating the Crabp2/Wnt/β-catenin signaling pathway, potentially providing a new treatment for DPN.

Correspondence to: Professor Dawei Yang, Department of Gerontology, Affiliated Hospital of Youjiang Medical University for Nationalities, 18 Zhongshan Road II, Baise, Guangxi Zhuang Autonomous Region 533099, P.R. China
E-mail: yangdaweisci@163.com

[*]Contributed equally

Key words: melittin, Schwann cells, diabetic peripheral neuropathy, proteomics, cellular retinoic acid binding protein 2/Wnt/β-catenin signaling pathway

Introduction

As one of the most common complications of diabetes, DPN refers to a condition in which patients with diabetes experience symptoms related to peripheral nerve dysfunction after other causes have been excluded (1). The symptoms of DPN primarily include abnormal sensations and pain in the extremities and increase the risk of amputation (2). Even strict blood sugar control can only reduce the incidence of DPN in type 1 diabetes, with little effect on type 2 diabetes (3). Currently, the main clinical approach for managing DPN is controlling blood sugar to alleviate symptoms, with few drugs available that specifically protect nerves (4). Therefore, finding new drugs and treatments is crucial.

Melittin (MLT) is a basic 26-amino acid polypeptide, making up 40-60% of dried bee venom (5). With advances in medical technology, MLT is now purified from bee venom, removing histamine and other harmful substances, which markedly reduces allergic reactions and toxic side effects, thus enhancing its clinical safety. Recent research has confirmed that MLT possesses anti-inflammatory properties, which can alleviate symptoms of dermatitis by inhibiting T cell-mediated inflammatory responses in mouse models (6). Additionally, several studies have demonstrated that MLT can reduce pain and promote nerve repair (7,8). It was hypothesized that MLT could also facilitate the repair of damaged nerves in DPN through these mechanisms, potentially improving neuropathy. The present study investigated the effects of MLT on the biological functions of SCs and identified the potential molecular mechanisms through which MLT enhances SC proliferation using TMT proteomic analysis, offering a novel approach for DPN treatment.

Materials and methods

Cell culture and drug purchase. RSC96 cells were obtained from Wuhan Punosai Life Technology Co., Ltd. These cells were cultured in DMEM (Gibco; Thermo Fisher Scientific, Inc.) containing 10% fetal bovine serum (Wuhan Punosai Life Technology Co., Ltd.) and maintained in a cell incubator at 37˚C with 5% CO_2. MLT was sourced from Selleck Chemicals.

Determination of glucose and MLT concentration. RSC96 cells were seeded into a 96-well plate at a density of $3x10^3$ cells per well. The glucose concentrations used were 2.8, 5.6, 7.0, 11.1, 16.9, 25, 33.3 and 50 mmol/l and the MLT concentrations were set at 0.05, 0.1, 0.2, 0.4, 0.8, 1.6 and 3.2 μg/ml. After 24, 48, and 72 h of treatment, 10 μl of CCK-8 reagent was added to each well, and the plates were incubated at 37˚C in a 5% CO_2 incubator for 1.5 h. The OD values at 450 nm were measured using a TriStar LB 941 multifunctional plate reader and cell viability was determined using a CCK-8 kit. Cell viability was calculated using the formula: [(As-Ab)/(Ac-Ab)] x100%, where As is the absorbance of the experimental well, Ab is the absorbance of the blank well and Ac is the absorbance of the control well.

Effect of MLT on SC cell activity in high glucose environment as detected by CCK-8. Experimental cells were divided into six groups: i) blank control group (NC); ii) high glucose model group (MC); iii) MLT low dose group [0.1 μg/ml, MLT(L) group]; iv) MLT medium dose group [0.2 μg/ml, MLT(M) group]; v) MLT high dose group [0.4 μg/ml, MLT(H) group]; and vi) positive control group (mecobalamin, MEC group). The experimental procedure involved adding $3x10^3$ cells per well/100 μl into 96-well plates and incubating them at 37˚C with 5% CO_2. After cell adhesion, the experimental and model groups were treated with high glucose for 24 h. The cells were then treated according to the aforementioned groups for 48 h, with five replicates per group. After the treatment period, 10 μl of CCK-8 reagent was added to each well, and the plates were incubated for 1.5 h. The OD values at 450 nm were measured using a plate reader, and the results were graphically represented using GraphPad Prism 8.0 software (Dotmatics).

Effects of MLT on SC cell cycle and apoptosis in high glucose environment analyzed by flow cytometry. The test model was established as described in *Effect of MLT on SC cell activity in high glucose environment as detected by CCK-8*. Cells were washed three times with PBS, and the cell concentration was adjusted to $1x10^5$/ml. A 1 ml single-cell suspension was collected, centrifuged (112 x g; 3 min; room temperature) and the supernatant was removed. The cells were fixed with 500 μl of cold 70% ethanol overnight and stored at 4˚C. Prior to staining, the fixing solution was washed off with PBS, the cell suspension was filtered through a 200-mesh screen and then the pre-prepared PI/RNase A staining working solution was added. Staining was conducted at room temperature, protected from light, for 30-60 min. Finally, the red fluorescence at an excitation wavelength of 488 nm was recorded for cell cycle analysis (ModFit LT, v5.0.9; Verity Software House) through flow cytometry using Invitrogen Attune NxT (Thermo Fisher Scientific, Inc.).

Cells were then treated with 5 μl of Annexin V-FITC, followed by 5 μl of propidium iodide, mixing each time. The reaction was allowed to proceed for 5-10 min at room temperature, protected from light. Following this, the cells in all groups were digested with trypsin without EDTA, washed twice with PBS, and apoptosis was detected within 1 h. Annexin V-FITC (Ex=488 nm, Em=530 nm) green fluorescence by FITC Channel (FL1) Detection; PI red fluorescence (Ex=488 nm, Em ≥630 nm) was detected by PI channels (FL2 or FL3). Then FlowJo (v10.8.1; FlowJo LLC) was used for data analysis. After flow cytometry data is imported into FlowJo, the software will directly calculate the proportion of normal cells (live cells), early apoptotic cells, late apoptotic cells and mechanically damaged cells in the total number of cells, so as to calculate the apoptosis rate of cells in each group (early + late apoptotic cells).

Proteomics combined with liquid chromatography-mass spectrometry analysis of protein expression in Schwann cells treated with MLT in high glucose environment. After 24 h of culture in a high glucose environment (25 mmol/l), RSC96 cells were treated with MLT (0.2 mg/ml) in the experimental group, while the control group was treated with high glucose medium only. After 48 h, proteins were extracted from both groups and analyzed using 4D label-free quantitative proteomics, with differences in protein expression identified using liquid chromatography-mass spectrometry (LC-MS). The process is divided into two parts: pre-experiment and formal experiment: Pre-experiment includes protein extraction, protein quantification, SDS-PAGE, protein enzymatic hydrolysis steps; The formal experiment is carried out on the basis of the pre-experiment and the samples qualified for quality control in the pre-experiment are formally tested by using high resolution mass spectrometer to obtain the original mass spectrum data. Samples were analyzed on a nanoElute (Bruker, Bremen, Germany) coupled to a timsTOF Pro (Bruker, Bremen, Germany) equipped with a CaptiveSpray source. The timsTOF Pro was operated in PASEF mode. Mass Range 100 to 1,700 m/z, 1/K0 start 0.75 V·s/cm^2 end 1.4 V·s/cm^2, ramp time 100 msec, Lock Duty Cycle to 100%, Capillary Voltage 1,500V, Dry Gas 3 l/min, Dry Temp 180˚C, PASEF settings: 10 MS/MS scans (total cycle time 1.16 sec), charge range 0-5, active exclusion for 0.5 min, Scheduling Target intensity 10,000, Intensity threshold 2,500, CID collision energy 20-59 eV.

Bioinformatics analysis. The raw files obtained from mass spectrometry were analyzed using database search software MaxQuant (1.6.17.0; Max-Planck-Institute of Biochemistry). Quality control assessments of peptide and protein levels were performed based on these search results, focusing on the repeatability of sample quantitation (Pearson correlation). Differential screening was then conducted based on the quantitative data, and statistical graphs illustrating these differences were generated. Differential proteins were functionally classified, including Gene Ontology (GO) secondary classification, Kyoto Encyclopedia of Genes and Genomes (KEGG) pathway analysis and domain annotation (9). Fisher's exact test was used for enrichment analysis, subcellular localization (WoLF PSORT, https://wolfpsort.hgc.jp/) and transcription factor analysis (AnimalTFDB 3.0, http://bioinfo.

Table I. Primers used for reverse transcription-quantitative PCR.

Gene	Primer sequence (5'-3')	Annealing temperature, ˚C
β-actin	Forward: TGTCACCAACTGGGACGATA	51.7
	Reverse: GGGGTGTTGAAGGTCTCAAA	51.7
Crabp2	Forward: GCCTAACTTTTCTGGCAACT	49.6
	Reverse: CCACAGCAATCTTCCTCAT	48.8
β-catenin	Forward: GGTGAAAATGCTTGGGTCG	51
	Reverse: CTGAAGGCAGTCTGTCGTA	51
PCNA	Forward: CTTGGAATCCCAGAACAGG	51
	Reverse: CTCGCAGAAAACTTCACCC	51
c-Jun	Forward: TGGGCACATCACCACTACA	51
	Reverse: TGACACTGGGCAGCGTATT	51
CDK4	Forward: ATTGGTGTCGGTGCCTATG	51
	Reverse: TCACGAACTGTGCTGACGG	49.1
Cyclind1	Forward: GGAGCAGAAGTGCGAAGA	50.2
	Reverse: GGGGCGGATAGAGTTGTC	52.5

life.hust.edu.cn/AnimalTFDB4/) of these proteins, as well as interaction network analysis for proteins showing significant variations (String; https://www.string-db.org/).

mRNA expression of related proteins as verified by reverse transcription-quantitative (RT-q) PCR. Total RNA was extracted and purified using the Monzol Reagent Pro (cat. no. MI20201S; Mona Biotechnology Co., Ltd.) kit, and primers were obtained from Wuhan Jinkairui Biotechnology Co., Ltd. Reverse transcription is then performed using MonScript RTIII All-in-One Mix with dsDNase. (cat. no. MR05101; Mona Biotechnology Co., Ltd.). The reverse transcription reaction conditions were set as follows: Incubation at 37˚C for 2 min to remove DNA contamination, followed by incubation at 55˚C for 15 min; the reaction was then terminated by heating at 85˚C for 5 min. MonAmp SYBR Green qPCR Mix (cat. no. MQ10101; Mona Biotechnology Co., Ltd.) was used for qPCR; the PCR reaction conditions included a pre-denaturation step at 95˚C for 30 sec, denaturation at 95˚C for 10 sec, annealing and extension at 60˚C for 30 sec, for 40 cycles. β-actin was used as the internal parameter, and the relative mRNA expression was calculated by $2^{-\Delta\Delta Cq}$ method (10). The primer gene sequences are shown in Table I.

Western blotting verification of the expression of related proteins. Cells from the specified groups were lysed using ultrasound (20 kHz; 4˚C; 1 min) and incubated on ice for 30 min. Following centrifugation at 12,000 x g at 4˚C for 10 min, the supernatant was collected. Protein concentration was determined using the BCA method, followed by 10% SDS-PAGE (10 μg protein loaded per lane) electrophoresis. Proteins were then transferred to membranes (0.45 μm PVDF; MilliporeSigma) by electrophoresis for 1.5 h and blocked with 5% skimmed milk powder at room temperature for 1 h. The primary antibodies used were cellular retinoic acid binding protein 2 (Crabp2; cat. no. ab211927; 1:1,000; Abcam), Wnt3a (cat. no. ab219412; 1:1,000; Abcam), β-catenin (cat. no. ab32572; 1:5,000; Abcam), c-Jun (cat. no. ab40766; 1:5,000; Abcam), CDK4 (cat. no. P24385; 1:1,000; Zen-Bio Inc.), CyclinD1 (cat. no. P11802; 1:1,000 Zen-Bio Inc.), proliferating cell nuclear antigen (PCNA; cat. no. R25294; 1:500; Zen-Bio Inc.) and β-Actin (cat. no. AF7018; 1:5,000; Affinity Biosciences, Ltd.). The membranes were incubated with the primary antibodies overnight on a shaker at 4˚C. The secondary antibody (cat. no. S0001; 1:1,000; Affinity Biosciences, Ltd.) was incubated at room temperature for 1 h, followed by three washes with TBST (0.1% Tween). Protein bands were visualized using the Yase Omni-ECL (Epizyme Biotech) ultra-sensitive chemiluminescence kit, and the grey values of each protein band were analyzed with ImageJ (v1.8.0; National Institutes of Health).

Statistical analysis. SPSS software (v26.0; IBM Corp.) was used to analyze the data, with each experiment conducted independently three times. Measurement data were expressed as mean ± standard deviation. An unpaired Student's t-test was used for comparisons between two groups, while one-way analysis of variance was used for comparisons among multiple groups, with pairwise tests performed for each group using Tukey's post hoc test. $P<0.05$ was considered to indicate a statistically significant difference.

Results

Determination of glucose and MLT concentration. Preliminary results indicated that after 24 h, cell activity peaked at a glucose concentration of 5.6 mmol/l. At a glucose concentration of 25 mmol/l, the inhibition rate of cell activity was highest (Fig. 1A). Consequently, 5.6 mmol/l glucose was selected for the blank control group, and 25 mmol/l for the model group (Fig. 1B). The survival rate of SCs cells under different concentration gradients of MLT was measured by CCK-8 method, thereby indirectly reflecting the proliferation of SCs. When the concentration of MLT was 0.2 μg/ml, the cell survival rate was the

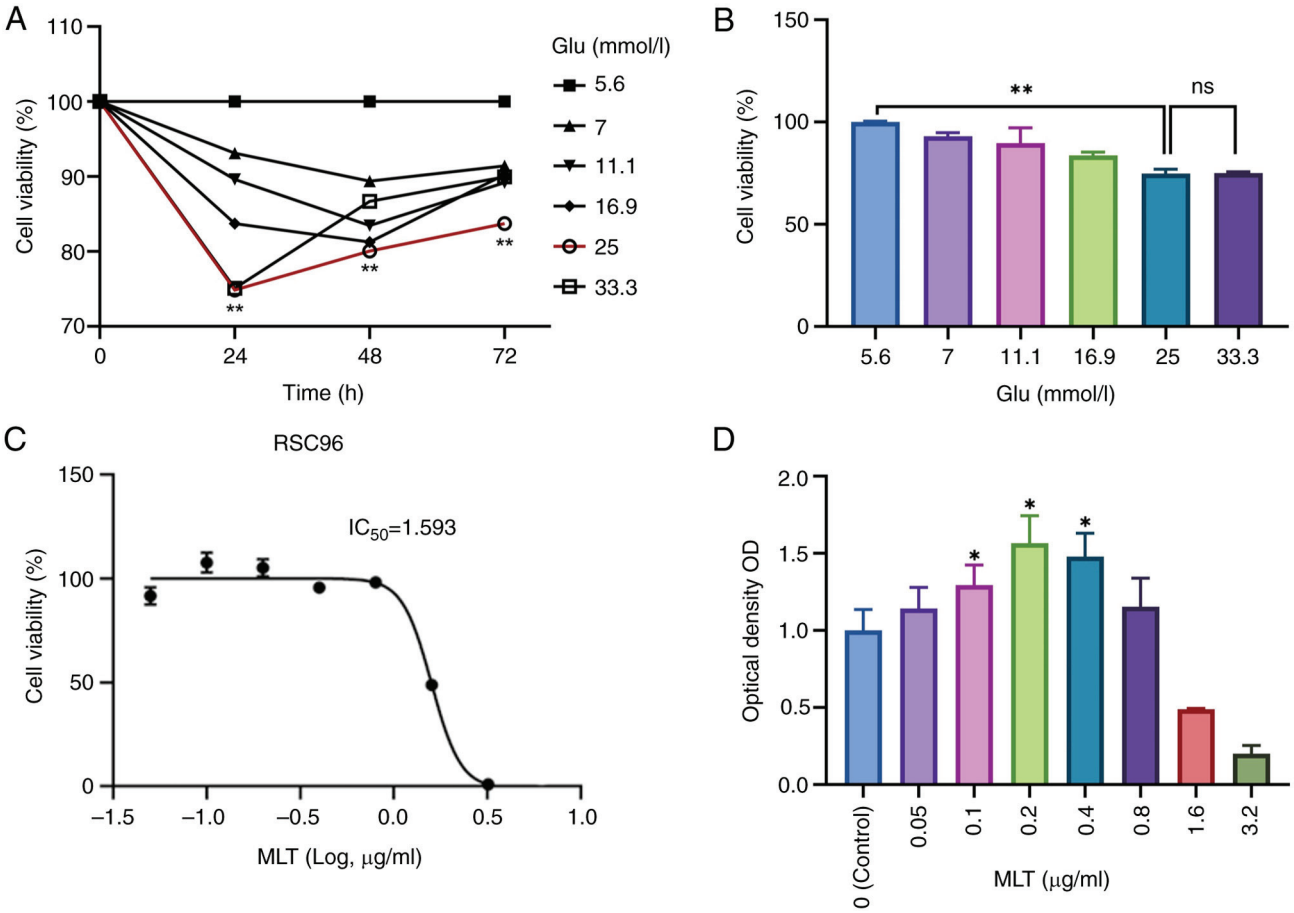

Figure 1. Glucose and MLT concentration (A) Survival rate of different concentrations of glucose in different time periods. (B) The effect of different glucose concentrations on cell viability during the optimal time period (24 h). (C) The IC_{50} curve of melittin. (D) Effects of different drug concentrations on cell viability. $^{*}P<0.05$, $^{**}P<0.01$.

highest. The survival rate was only 50% at 1.6 μg/ml, and even lower at 3.2 μg/ml (Fig. 1D). Therefore, three concentrations of MLT within the IC_{50} range were selected for the experimental group, and cell proliferation factor was detected by western blotting and immunofluorescence. Compared with the model group, the expression of cell proliferation factor was increased in the MLT group, so that MLT within a certain concentration range could promote the proliferation of SCs in a high-sugar environment. Under high glucose conditions, when the concentration of MLT was 0.2 μg/l and the incubation time was 48 h, cell activity reached its maximum, and the IC_{50} was calculated (Fig. 1C). Concentrations of 0.1, 0.2, and 0.4 μg/ml were ultimately chosen as the low, medium, and high concentrations of MLT, respectively (Fig. 1D).

MLT promotes the proliferation of Schwann cells and inhibits the apoptosis of Schwann cells in high glucose environment. After 24 h of culturing RSC96 cells in high glucose conditions, different concentrations of MLT were administered to each group, and cell activity was measured using the CCK-8 assay (Fig. 2A). The results showed that the medium concentration of MLT had the highest cell survival rate. PCR (Fig. 2B) and western blotting analysis (Fig. 2C) were then used to assess the expression of PCNA. Compared with the model group, PCNA expression in Schwann cells treated with MLT increased, supporting the CCK-8 findings. In western blotting analysis, the difference in PCNA expression between the low, medium, and high concentrations of MLT was not significant, with the MLT(M) showing slightly higher expression than the other two groups. Flow cytometry showed that the combined rates of early and late apoptosis in the MLT group were lower than those in the model group (Fig. 2D). In summary, MLT promoted SC proliferation and reduced SC apoptosis in a high glucose environment. Additionally, the fluorescence intensity of Ki-67 was measured using immunofluorescence. The fluorescence intensity of Ki-67 was significantly higher in the control group than in the model group and it increased further in the MLT(M) group (Fig. 2E).

Proteomic analysis

Consistency test of mouse Schwann cell protein samples. Based on the aforementioned findings, 4D label-free quantitative proteomic analysis was conducted on MLT-treated and untreated SCs to generate proteomic data for bioinformatics analysis. The results from the protein quantitative principal component analysis indicated high quantitative repeatability among replicates, with significant differences between the two groups (Fig. 3A). The Pearson correlation coefficient between samples was close to 1, indicating excellent sample repeatability (Fig. 3B). Additionally, the relative standard

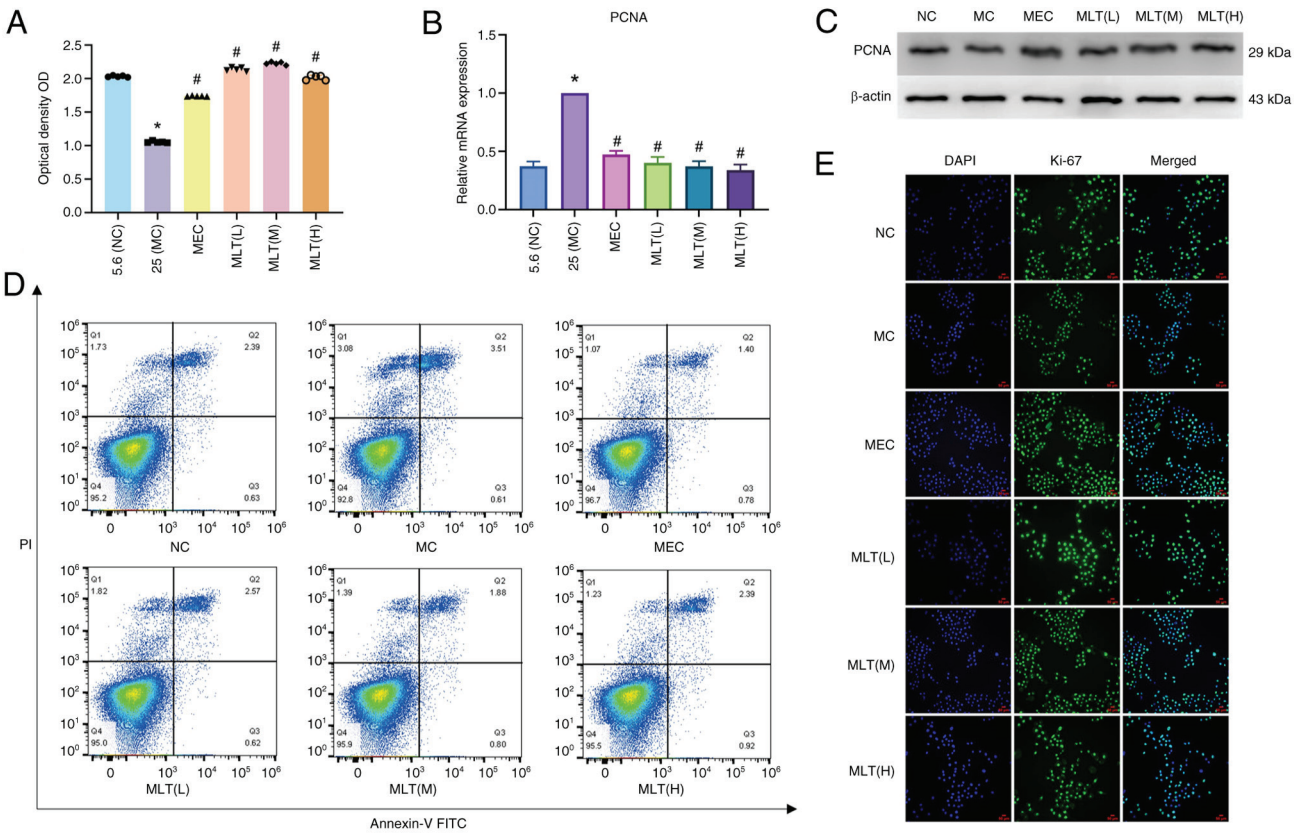

Figure 2. Effects of MLT on Schwann cell proliferation and apoptosis. (A) Following MLT treatment, the cell viability of control group (Glu 5.6 mmol/l), model group (Glu 25 mmol/l), positive control group (mecobalamine) and the low, medium and high concentrations of MLT for 48 h were determined. (B) The mRNA expression of PCNA of RSC96 cells in each group). (C) The protein expression level of PCNA in RSC96 cells in each group; (D and E) Ki-67 was stained, and the subcellular localization and expression of Ki-67 in each group were observed by confocal microscopy (scale bar, 50 μm). *P<0.05 vs. control group; #P<0.05 vs. model group. MLT, melittin; Glu, glucose; MEC, mecobalamine; NC, negative control; PCNA, proliferating cell nuclear antigen; MC, high glucose model group; NC, negative control.

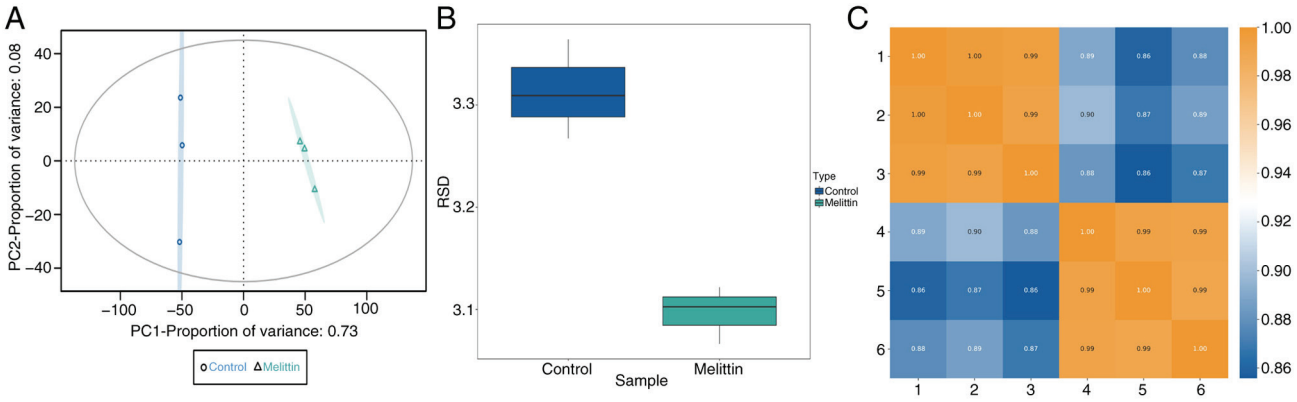

Figure 3. Proteomic results. (A) Principal component analysis. (B) Relative standard deviation of protein quantitative values between samples. (C) Pearson's correlation coefficient analysis.

deviation of protein quantitative values between samples was low, confirming the robust quantitative repeatability of the proteomics data (Fig. 3C).

4D labeling free quantitative proteomic analysis performed on the groups using proteomic data. Samples of rat cells were analyzed using high-throughput, label-free LC-MS/MS. Proteins with a FC greater than 1.5 were selected, indicating statistically significant differences in differentially expressed proteins (DEPs) between the two groups with P<0.05.

Compared with the control group, the experimental group showed 1,784 DEPs, with 725 upregulated proteins. These differences were statistically significant (Fig. 4A). The ten most upregulated proteins included Crabp2, S100a4, Necap2, Pea15, Nmral1, Pgls, Gnpnat1, Amdhd2, Helz, MvdCrabp2, S100a4, adaptin ear-binding coat-associated protein 2, Astrocytic phosphoprotein PEA-15, NmrA-like family domain-containing protein 1,6-phosphogluconolactonase, glucosamine-phosphate N-acetyltransferase 1, N-acetylglucosamine-6-phosphate deacetylase, probable helicase with zinc finger domain and

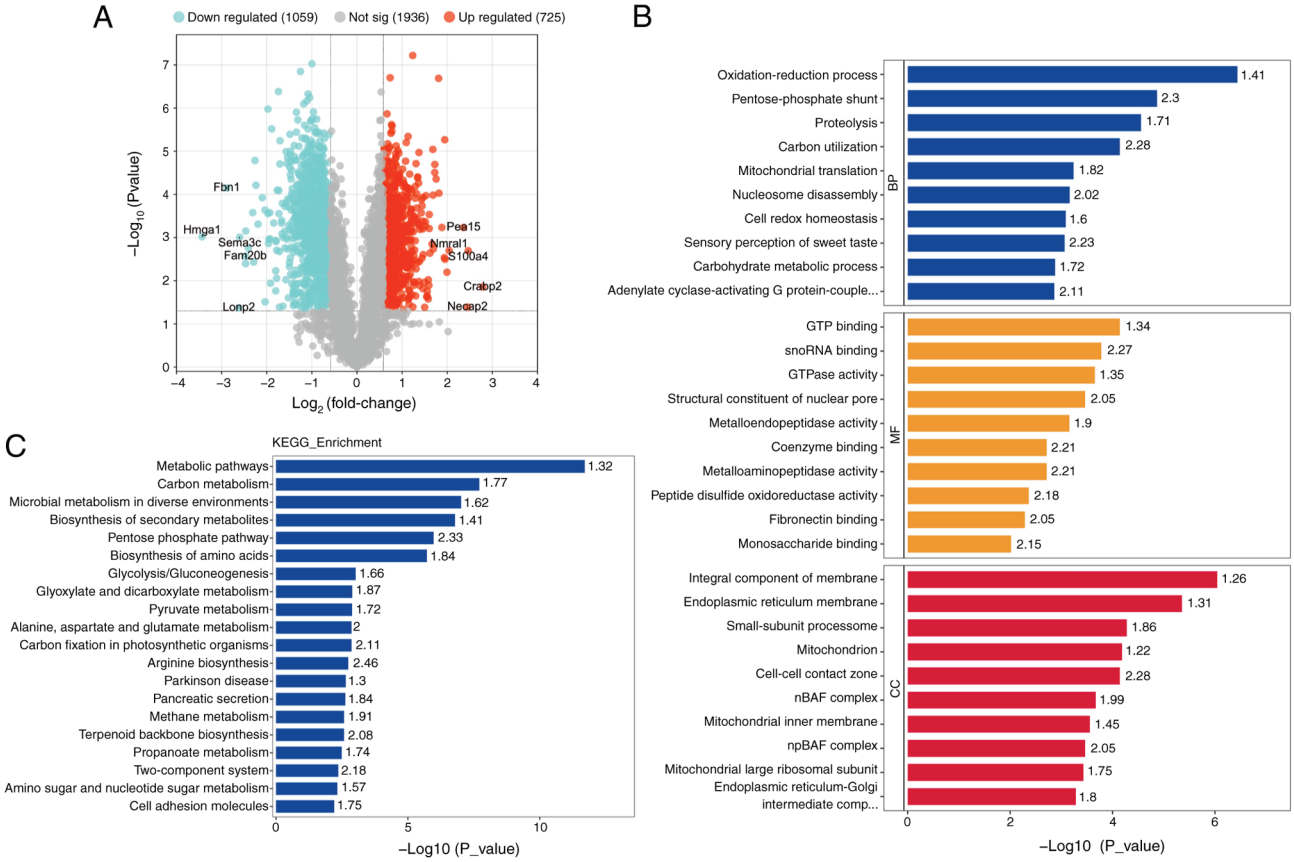

Figure 4. Differential protein screening and KEGG, GO enrichment analysis. (A) The results of differential protein screening were presented in the form of volcano plot. (B) KEGG Pathway Annotation. (C) GO Annotation. GO, Gene Ontology; KEGG, Kyoto Encyclopedia of Genes and Genomes; Hmga1, high mobility group protein HMG-I/HMG-Y; Fbn1, fibrillin-1; Lonp2, Lon protease homolog 2 peroxisomal; Sema3c, semaphorin 3C; Fam20b, glycosaminoglycan xylosylkinase; Atad2, ATPase family AAA domain containing protein 2; Abcc4, ATP-binding cassette sub-family C member 4; Itpr1, inositol 1,4,5-trisphosphate receptor type 1; Exd2, exonuclease 3'-5' domain-containing protein 2; Lrrc8e, volume-regulated anion channel subunit LRRC8E; Crabp2, cellular retinoic acid binding protein 2; Necap2, adaptin ear-binding coat-associated protein 2; Pea15, astrocytic phosphoprotein PEA-15; Nmral1, NmrA-like family domain-containing protein 1; Pgls, 6-phosphogluconolactonase; Gnpnat1, glucosamine-phosphate N-acetyltransferase 1; Amdhd2, N-acetylglucosamine-6-phosphate deacetylase, Helz, probable helicase with zinc finger domain; Mvd, diphosphomevalonate decarboxylase.

diphosphomevalonate decarboxylase, while the 10 most downregulated proteins included high mobility group protein HMG-I/HMG-Y, fibrillin-1, Lon protease homolog 2 peroxisomal, semaphorin 3C, glycosaminoglycan xylosylkinase, ATPase family AAA domain containing protein 2, ATP-binding cassette sub-family C member 4, inositol 1,4,5-trisphosphate receptor type 1, exonuclease 3'-5' domain-containing protein 2 and volume-regulated anion channel subunit LRRC8E. GO secondary annotation revealed that most DEPs had binding and catalytic activities at the molecular functional level. KEGG pathway analysis indicated that these proteins were involved in metabolic pathways, pathways related to neurodegeneration in multiple diseases, Parkinson's disease and Huntington's disease. GO functional enrichment analysis showed significant trends in enzyme regulation functions, such as GTP binding and GTPase activity (Fig. 4B). The top 10 KEGG pathways were illustrated (Fig. 4C). Protein domains, which are regions with specific structures and independent functions within proteins, were also analyzed and depicted in a circular graph (Fig. 5A). Subcellular localization analysis using WoLF PSORT indicated that most DEPs were primarily located in the cytoplasm (30%) and nucleus (27.9%) (Fig. 5B). Additionally, direct and indirect interaction network analyses were conducted on 23 significantly different proteins, with the direct interaction network plotted (Fig. 5C).

MLT prevents cell stasis by altering the cell cycle. Western blotting (Fig. 6A) and PCR (Fig. 6C) were used to detect cell cycle-related factors. Compared with the model group, the expression of CDK4 and CyclinD1 was increased in the experimental group. Flow cytometry showed that the G_2/M+S phase was prolonged in the MLT(L), MLT(M) and MLT(H) groups vs. the model group, with the most pronounced effect in the MLT(M) group (Fig. 6B).

MLT promotes SCs proliferation through up-regulation of Crabp2/Wnt/β-catenin signaling pathway. Proteomic analysis revealed that Crabp2 was significantly upregulated among various proteins. Western blotting (Fig. 7A), immunofluorescence (Fig. 7B) and RT-qPCR (Fig. 7C) confirmed the increased expression of Crabp2 in MLT-treated SCs, particularly in the MLT(M) group. Crabp2 has been shown to activate the Wnt/β-catenin pathway (11). PCR and western blotting were used to detect factors related to the Wnt/β-catenin pathway, revealing that MLT treatment increased the expression of Wnt3a, β-catenin, and c-Jun in SCs, thereby activating the

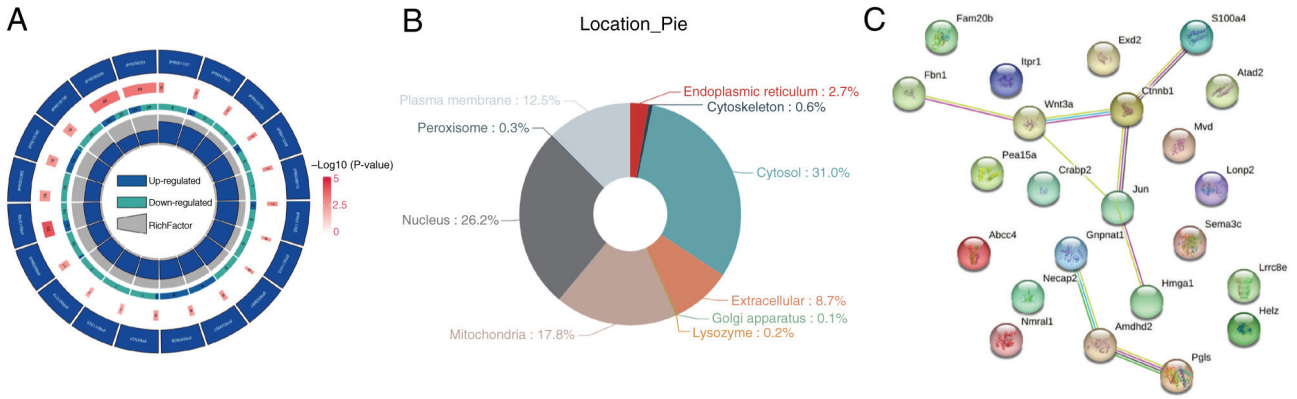

Figure 5. Domain enrichment, subcellular localization, and PPI. (A) The results of differential protein domain annotation were enriched and analyzed, and the results were displayed in the form of a circle graph. (B) Protein subcellular localization map. (C) target protein direct interaction network.

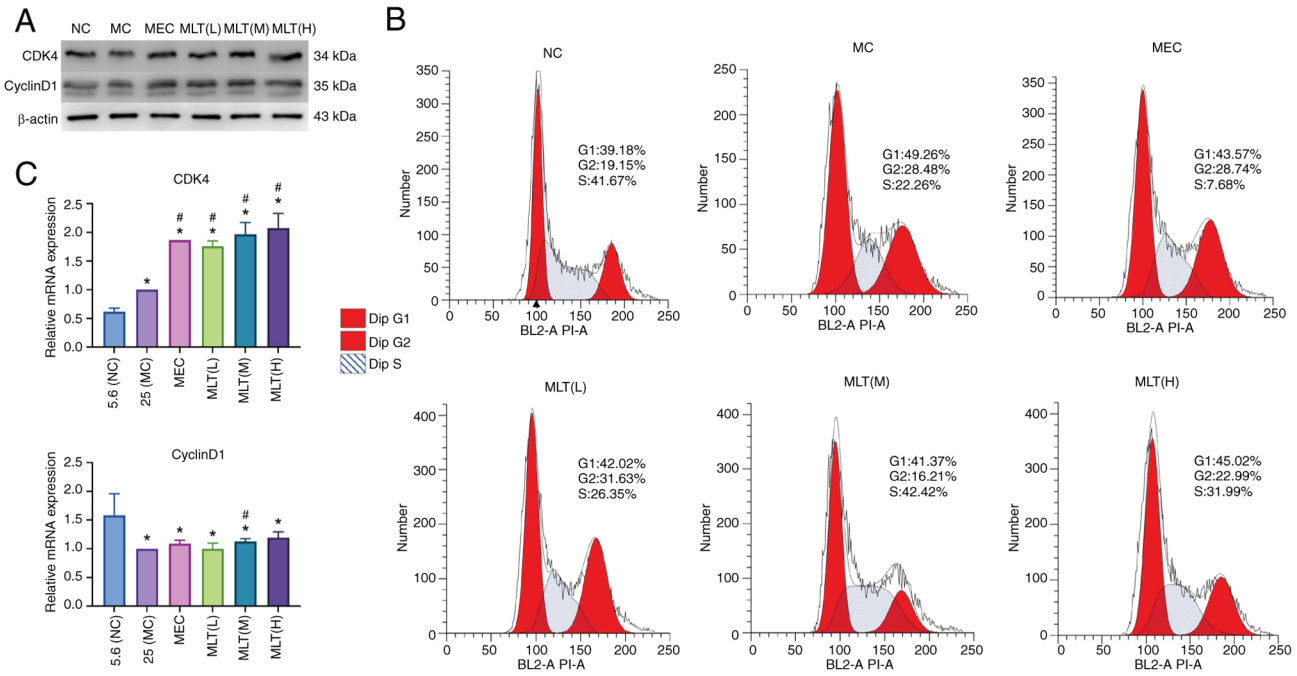

Figure 6. Effect of melittin on cell cycle. (A) The protein expression level of CDK4 and Cyclind1 in RSC96 cells in each group. (B) The cell cycle of each group was detected by flow cytometry. (C) The mRNA expression level of CDK4 and Cyclind1 in RSC96 cells in each group. *P<0.05 vs. control group, #P<0.05 vs. model group. MC, high glucose model group; NC, negative control; MEC, mecobalamine; MLT, melittin; PCNA, proliferating cell nuclear antigen.

Wnt/β-catenin pathway. The results were consistent across the MLT groups, with no significant differences observed. Further verification of Crabp2 expression post-MLT treatment using immunofluorescence confirmed these findings.

Discussion

Numerous studies have explored diabetic peripheral neuropathy (DPN), but the precise mechanisms remain unclear. Previous research suggests links to various metabolic pathways, including the polyol pathway, hexosamine pathway, advanced glycosylation end products, oxidative stress and nerve growth factor (12-14). These factors are important for understanding the pathological processes in peripheral neurons under diabetic conditions. Notably, most clinical and basic research on DPN has focused on the neuronal aspects, viewing neurons as the primary signal-transmitting elements. However, extensive data on the development and regeneration of the peripheral nervous system emphasize the critical role of glial cells in supporting neuronal structure and function, nourishing axons (15-17) and aiding in survival and growth after injury (18).

SCs play a crucial role in nerve regeneration following peripheral nerve injury. They enhance the repair capabilities of various tissues, dedifferentiate after injury, and secrete neurotrophic factors such as Glial cell line-derived neurotrophic factor (GDNF), nerve growth factor (NGF), brain derived neurotrophic factor (BDNF) and ciliary neurotrophic factor (CNTF), which support nerve fiber regeneration (19). SCs also interact with other cells, such as fibroblasts and macrophages, to clear myelin debris from damaged nerves, create paths for regeneration and repair nerves (20,21). Although it remains debated whether the primary lesion in DPN is

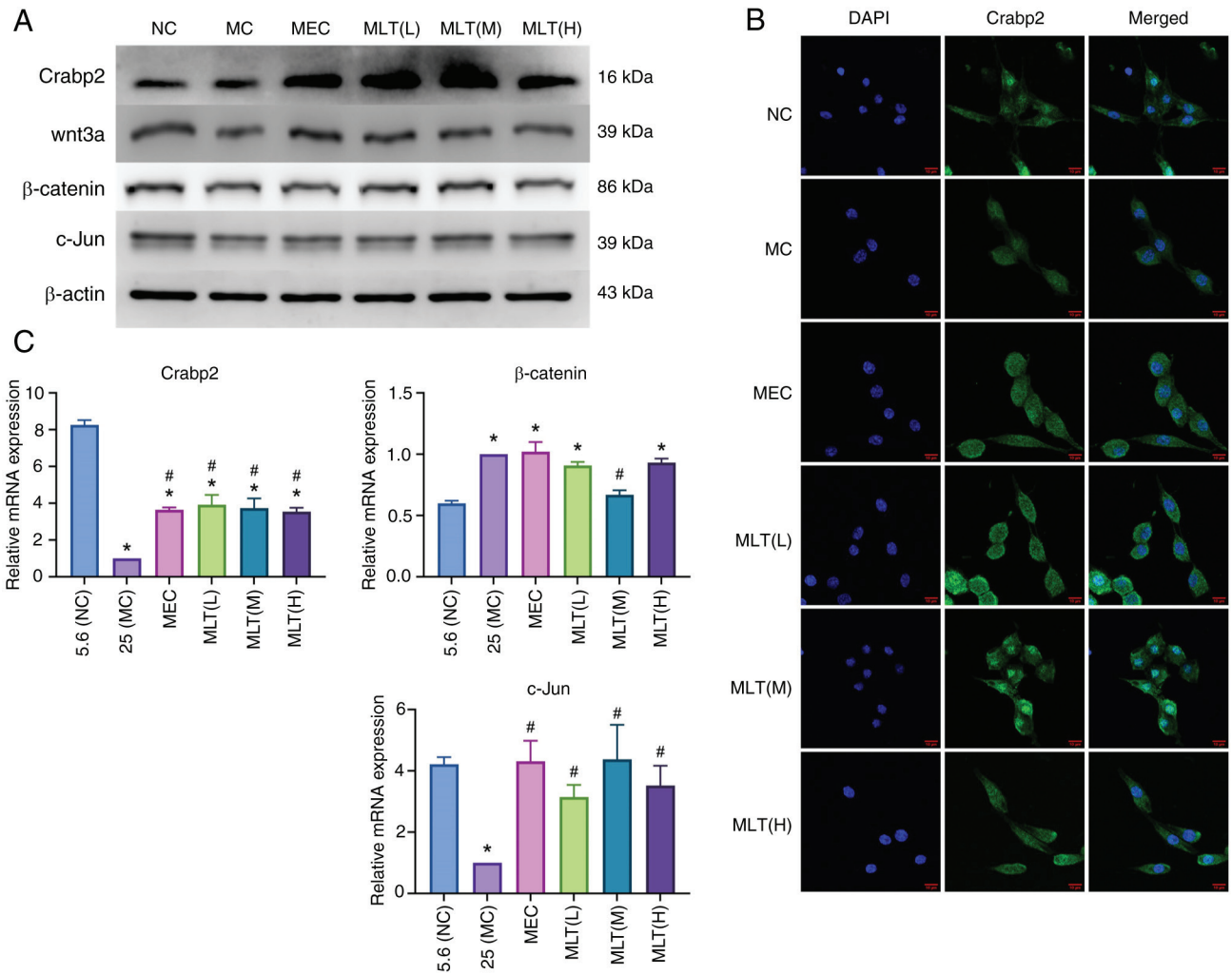

Figure 7. The mechanism of MLT promoting cell proliferation. (A) The protein expression level of Crabp2, Wnt3a, β-catenin and c-Jun in RSC96 cells in each group. (B) The subcellular localization and expression of Crabp2 in each group were observed by confocal microscopy, scale bar, 10 μm. (C) The mRNA expression level of Crabp2, Wnt3a, β-catenin and c-Jun in RSC96 cells in each group (*P<0.05 vs. control group, $^{\#}$P<0.05 vs. model group. Crabp2, cellular retinoic acid; NC, negative control; MC, high glucose model group; MEC, mecobalamine; MLT, melittin.

demyelination or axon loss, SCs are now recognized as central to the pathogenesis of DPN (22).

MLT, a water-soluble cationic peptide derived from bee venom, is widely used in the treatment of various cancers (23-25). Its anti-inflammatory and analgesic properties have also been applied to treat peripheral neuropathy caused by chemotherapy (26-28). The mechanism involves the activation of intracellular signaling pathways, promotion of cell proliferation and inhibition of apoptosis.

The present study first examined cell viability in response to varying glucose concentrations over different time periods. It was found that the effect of high glucose concentrations on cell viability was most pronounced at 25 and 33.3 mmol/l after 24 h, but this effect diminished after 48 and 72 h. This reduction may be due to nutrient depletion, such as glucose, during prolonged cell growth, leading to lower glucose levels in the medium than initially provided. Therefore, the 24-h time point was chosen as it accurately and efficiently reflects cell vitality under high glucose conditions. Three concentrations of MLT within its IC_{50} range were then selected for the experimental group. The results showed that MLT promotes SC proliferation and inhibits apoptosis *in vitro*, suggesting a potential therapeutic mechanism for MLT in treating DPN.

To further explore the underlying mechanisms, TMT labeling quantitative proteomics and bioinformatics analysis were used. The proteomic analysis identified 1,784 DEPs after MLT treatment, with 725 upregulated and 1,059 downregulated. GO annotation and functional enrichment analysis indicated that a number of these proteins were involved in protein binding, RNA binding, GTP binding, GTPase activity, and redox processes, all of which are closely associated with the onset of DPN (29). KEGG pathway analysis suggested that the effects of MLT might be linked to various metabolic pathways, including amino sugar and nucleotide sugar metabolism, neurodegenerative disease pathways, and protein processing in the endoplasmic reticulum, all of which are important in the development of DPN (30,31).

Among the identified proteins, Crabp2 was the most significantly upregulated. Crabp2 belongs to the intracellular lipid-binding protein family and acts as a shuttle protein between the cytoplasm and nucleus. It is primarily found in the skin, uterus, ovary and nerve choroid (32). Crabp2 is closely linked to neurological disorders (33). It can activate the Wnt/β-catenin

signaling pathway, promoting the proliferation of Hu sheep dermal papilla cells (DPCs) (11). The Wnt/β-catenin signaling pathway plays a vital role in the development of nervous system-related diseases (34,35). While this pathway typically becomes inactive after embryonic development, it can reactivate in adults to promote nerve repair after injury (36). For example, injecting Wnt3a into the vitreous of mice has been shown to facilitate the regeneration of retinal ganglion cell axons, indicating that Wnt3a activates the Wnt/β-catenin pathway to aid nerve repair when ganglion cells are damaged (37). In diabetes, hyperglycemia can lead to the demyelination of peripheral nerve fibers, activating the Wnt/β-catenin pathway. However, prolonged hyperglycemia can result in damage that outpaces repair, leading to peripheral nerve demyelination and axonal degeneration, which contribute to DPN (38).

In the present study, MLT treatment of SCs led to a significant increase in Crabp2 expression and the upregulation of the Wnt/β-catenin signaling pathway. Inhibition of GSK-3β prevents the degradation of β-Catenin, allowing it to enter the nucleus and initiate the transcription of downstream genes, including c-Jun. c-Jun directly regulates the transcription of CyclinD1, promoting cell proliferation by facilitating the G_1 phase of the cell cycle (39-41). In the present study, the expression of the cell cycle-dependent complex CDK4/CyclinD1, essential for the transition from G_1 to S phase, was increased. Flow cytometry results indicated that MLT treatment significantly decreased the proportion of cells in the G_0/G_1 phase, while increasing the number in the G_2/M and S phases. This shift suggested that MLT inhibited the transition from proliferation to differentiation, thereby promoting cell proliferation (42,43). In summary, MLT may protect cells from hyperglycemic toxicity and enhance SC proliferation by upregulating Crabp2 expression, activating the Wnt/β-catenin signaling pathway and shortening the cell cycle.

Currently, research on MLT therapy is limited both domestically and internationally, with few studies examining its role in DPN. The present study introduced the innovative use of proteomics to analyze the expression of DEPs in SCs treated with MLT under high-glucose conditions. It explored the mechanism by which MLT may treat DPN, providing valuable experimental insights for further research in MLT-related fields and laying a theoretical foundation for its clinical application in DPN treatment. In the future, it is possible that MLT could be administered through acupuncture points or topical applications to alleviate the symptoms of DPN. However, the present study has limitations due to its *in vitro* nature; further animal experiments are necessary to validate its findings. Additionally, due to financial constraints, only the RSC96 cell line was used. According to literature, the RSC96 cell line is commonly used in peripheral neuropathy research, giving it a degree of representativeness. In future studies, more cell lines may be included.

Acknowledgements

Not applicable.

Funding

The present study was supported by the Guangxi Natural Science Foundation project (grant no. 2020JJA140216), Guangxi medical and health self-financing plan (grant no. Z20170240).

Availability of data and materials

The data generated in the present study may be requested from the corresponding author.

Author's contributions

QZ was responsible conceptualization, writing the original draft, software and diagrams, reviewing and editing. YC was responsible for software and formal analysis. WH was responsible for software, resources, data curation and acquisition of data. JZ was responsible for software and analysis and interpretation of data. DY was responsible for conceptualization, methodology, writing, review and editing, supervision, project administration and funding acquisition. QZ and DY confirm the authenticity of all the raw data. All authors read and approved the final manuscript.

Ethics approval and consent to participate

Not applicable.

Patient consent for publication

Not applicable.

Competing interests

The authors declare that they have no competing interests.

References

1. Selvarajah D, Kar D, Khunti K, Davies MJ, Scott AR, Walker J and Tesfaye S: Diabetic peripheral neuropathy: Advances in diagnosis and strategies for screening and early intervention. Lancet Diabetes Endocrinol 7: 938-948, 2019.
2. Sun H, Saeedi P, Karuranga S, Pinkepank M, Ogurtsova K, Duncan BB, Stein C, Basit A, Chan JCN, Mbanya JC, *et al*: IDF diabetes atlas: Global, regional and country-level diabetes prevalence estimates for 2021 and projections for 2045. Diabetes Res Clin Pract 183: 109119, 2022.
3. Calcutt NA: Diabetic neuropathy and neuropathic pain: A (con) fusion of pathogenic mechanisms? Pain 161 (Suppl 1): S65-S86, 2020.
4. Sloan G, Selvarajah D and Tesfaye S: Pathogenesis, diagnosis and clinical management of diabetic sensorimotor peripheral neuropathy. Nat Rev Endocrinol 17: 400-420, 2021.
5. Memariani H and Memariani M: Melittin as a promising anti-protozoan peptide: Current knowledge and future prospects. AMB Express 11: 69, 2021.
6. Liu Z, Fan Z, Liu J, Wang J, Xu M, Li X, Xu Y, Lu Y, Han C and Zhang Z: Melittin-carrying nanoparticle suppress T cell-driven immunity in a murine allergic dermatitis model. Adv Sci (Weinh) 10: e2204184, 2023.
7. Choi S, Chae HK, Heo H, Hahm DH, Kim W and Kim SK: Analgesic effect of melittin on oxaliplatin-induced peripheral neuropathy in rats. Toxins (Basel) 11: 396, 2019.
8. Shaik RA, Alotaibi MF, Nasrullah MZ, Alrabia MW, Asfour HZ and Abdel-Naim AB: Cordycepin-melittin nanoconjugate intensifies wound healing efficacy in diabetic rats. Saudi Pharm J 31: 736-745, 2023.
9. Dennis G, Sherman BT, Hosack DA, Yang J, Gao W, Lane HC and Lempicki RA: DAVID: Database for annotation, visualization, and integrated discovery. Genome Biol 4: P3, 2003.

10. Livak KJ and Schmittgen TD: Analysis of relative gene expression data using real-time quantitative PCR and the 2(-Delta Delta C(T)) method. Methods 25: 402-408, 2001.
11. He M, Lv X, Cao X, Yuan Z, Quan K, Getachew T, Mwacharo JM, Haile A, Li Y, Wang S and Sun W: CRABP2 promotes the proliferation of dermal papilla cells via the Wnt/β-catenin pathway. Animals (Basel) 13: 2033, 2023.
12. Baum P, Toyka KV, Blüher M, Kosacka J and Nowicki M: Inflammatory mechanisms in the pathophysiology of diabetic peripheral neuropathy (DN)-new aspects. Int J Mol Sci 22: 10835, 2021.
13. Eftekharpour E and Fernyhough P: Oxidative stress and mitochondrial dysfunction associated with peripheral neuropathy in type 1 diabetes. Antioxid Redox Signal 37: 578-596, 2022.
14. Rumora AE, Kim B and Feldman EL: A Role for fatty acids in peripheral neuropathy associated with type 2 diabetes and prediabetes. Antioxid Redox Signal 37: 560-577, 2022.
15. Yang C, Zhao X, An X, Zhang Y, Sun W, Zhang Y, Duan Y, Kang X, Sun Y, Jiang L and Lian F: Axonal transport deficits in the pathogenesis of diabetic peripheral neuropathy. Front Endocrinol (Lausanne) 14: 1136796, 2023.
16. Majd H, Amin S, Ghazizadeh Z, Cesiulis A, Arroyo E, Lankford K, Majd A, Farahvashi S, Chemel AK, Okoye M, *et al*: Deriving Schwann cells from hPSCs enables disease modeling and drug discovery for diabetic peripheral neuropathy. Cell Stem Cell 30: 632-647.e10, 2023.
17. Wang X, Xu G, Liu H, Chen Z, Huang S, Yuan J, Xie C and Du L: Inhibiting apoptosis of Schwann cell under the high-glucose condition: A promising approach to treat diabetic peripheral neuropathy using Chinese herbal medicine. Biomed Pharmacother 157: 114059, 2023.
18. Cheng Y, Liu J, Luan Y, Liu Z, Lai H, Zhong W, Yang Y, Yu H, Feng N, Wang H, *et al*: Sarm1 gene deficiency attenuates diabetic peripheral neuropathy in mice. Diabetes 68: 2120-2130, 2019.
19. Wang Q, Chen FY, Ling ZM, Su WF, Zhao YY, Chen G and Wei ZY: The effect of Schwann cells/schwann cell-like cells on cell therapy for peripheral neuropathy. Front Cell Neurosci 16: 836931, 2022.
20. Kalinski AL, Yoon C, Huffman LD, Duncker PC, Kohen R, Passino R, Hafner H, Johnson C, Kawaguchi R, Carbajal KS, *et al*: Analysis of the immune response to sciatic nerve injury identifies efferocytosis as a key mechanism of nerve debridement. Elife 9: e60223, 2020.
21. Qu WR, Zhu Z, Liu J, Song DB, Tian H, Chen BP, Li R and Deng LX: Interaction between Schwann cells and other cells during repair of peripheral nerve injury. Neural Regen Res 16: 93-98, 2021.
22. Chen CZ, Neumann B, Förster S and Franklin RJM: Schwann cell remyelination of the central nervous system: Why does it happen and what are the benefits? Open Biol 11: 200352, 2021.
23. Han IH, Jeong C, Yang J, Park SH, Hwang DS and Bae H: Therapeutic effect of melittin-dKLA targeting tumor-associated macrophages in melanoma. Int J Mol Sci 23: 3094, 2022.
24. Yu X, Dai Y, Zhao Y, Qi S, Liu L, Lu L, Luo Q and Zhang Z: Melittin-lipid nanoparticles target to lymph nodes and elicit a systemic anti-tumor immune response. Nat Commun 11: 1110, 2020.
25. Ombredane AS, de Andrade LR, Bonadio RS, Pinheiro WO, de Azevedo RB and Joanitti GA: Melittin sensitizes skin squamous carcinoma cells to 5-fluorouracil by affecting cell proliferation and survival. Exp Dermatol 30: 710-716, 2021.
26. Fan XG, Pei SY, Zhou D, Zhou PC, Huang Y, Hu XW, Li T, Wang Y, Huang ZB and Li N: Melittin ameliorates inflammation in mouse acute liver failure via inhibition of PKM2-mediated Warburg effect. Acta Pharmacol Sin 42: 1256-1266, 2021.
27. Tender T, Rahangdale RR, Balireddy S, Nampoothiri M, Sharma KK and Raghu Chandrashekar H: Melittin, a honeybee venom derived peptide for the treatment of chemotherapy-induced peripheral neuropathy. Med Oncol 38: 52, 2021.
28. Er-Rouassi H, Bakour M, Touzani S, Vilas-Boas M, Falcão S, Vidal C and Lyoussi B: Beneficial effect of bee venom and its major components on facial nerve injury induced in mice. Biomolecules 13: 680, 2023.
29. Mandel N, Büttner M, Poschet G, Kuner R and Agarwal N: SUMOylation modulates reactive oxygen species (ROS) levels and acts as a protective mechanism in the type 2 model of diabetic peripheral neuropathy. Cells 12: 2511, 2023.
30. Pang B, Zhang LL, Li B, Sun FX and Wang ZD: BMP5 ameliorates diabetic peripheral neuropathy by augmenting mitochondrial function and inhibiting apoptosis in Schwann cells. Biochem Biophys Res Commun 643: 69-76, 2023.
31. Hu Y, Chen C, Liang Z, Liu T, Hu X, Wang G, Hu J, Xie X and Liu Z: Compound Qiying Granules alleviates diabetic peripheral neuropathy by inhibiting endoplasmic reticulum stress and apoptosis. Mol Med 29: 98, 2023.
32. Larange A, Takazawa I, Kakugawa K, Thiault N, Ngoi S, Olive ME, Iwaya H, Seguin L, Vicente-Suarez I, Becart S, *et al*: A regulatory circuit controlled by extranuclear and nuclear retinoic acid receptor α determines T cell activation and function. Immunity 56: 2054-2069.e10, 2023.
33. Khazeem MM, Casement JW, Schlossmacher G, Kenneth NS, Sumbung NK, Chan JYT, McGow JF, Cowell IG and Austin CA: TOP2B is required to maintain the adrenergic neural phenotype and for ATRA-induced differentiation of SH-SY5Y neuroblastoma cells. Mol Neurobiol 59: 5987-6008, 2022.
34. Kim TW, Piao J, Koo SY, Kriks S, Chung SY, Betel D, Socci ND, Choi SJ, Zabierowski S, Dubose BN, *et al*: Biphasic activation of WNT signaling facilitates the derivation of midbrain dopamine neurons from hESCs for translational use. Cell Stem Cell 28: 343-355.e5, 2021.
35. Sun X, Peng X, Cao Y, Zhou Y and Sun Y: ADNP promotes neural differentiation by modulating Wnt/β-catenin signaling. Nat Commun 11: 2984, 2020.
36. Gao J, Liao Y, Qiu M and Shen W: Wnt/β-catenin signaling in neural stem cell homeostasis and neurological diseases. Neuroscientist 27: 58-72, 2021.
37. Jang E, Jin S, Cho KJ, Kim D, Rho CR and Lyu J: Wnt/β-catenin signaling stimulates the self-renewal of conjunctival stem cells and promotes corneal conjunctivalization. Exp Mol Med 54: 1156-1164, 2022.
38. El-Sawaf ES, Saleh S, Abdallah DM, Ahmed KA and El-Abhar HS: Vitamin D and rosuvastatin obliterate peripheral neuropathy in a type-2 diabetes model through modulating Notch1, Wnt-10α, TGF-β and NRF-1 crosstalk. Life Sci 279: 119697, 2021.
39. Kullmann MK, Pegka F, Ploner C and Hengst L: Stimulation of c-Jun/AP-1-activity by the cell cycle inhibitor $p57^{Kip2}$. Front Cell Dev Biol 9: 664609, 2021.
40. Requejo-Aguilar R: Cdk5 and aberrant cell cycle activation at the core of neurodegeneration. Neural Regen Res 18: 1186-1190, 2023.
41. Chen Z, Xie Y, Luo H, Song Y, Que T, Hu R, Huang H, Luo K, Li C, Qin C, *et al*: NAP1L1 promotes proliferation and chemoresistance in glioma by inducing CCND1/CDK4/CDK6 expression through its interaction with HDGF and activation of c-Jun. Aging (Albany NY) 13: 26180-26200, 2021.
42. Lange C, Huttner WB and Calegari F: Cdk4/cyclinD1 overexpression in neural stem cells shortens G1, delays neurogenesis, and promotes the generation and expansion of basal progenitors. Cell Stem Cell 5: 320-331, 2009.
43. Gao S, Tan H and Gang J: Inhibition of hepatocellular carcinoma cell proliferation through regulation of the cell cycle, AGE-RAGE, and Leptin signaling pathways by a compound formulation comprised of andrographolide, wogonin, and oroxylin A derived from andrographis paniculata(Burm.f.) nees. J Ethnopharmacol 329: 118001, 2024.